

Causal Image Synthesis of Brain MR in 3D

Yujia Li^{1,3}, Jiong Shi^{4,5}, and S. Kevin Zhou^{1,2,3}

¹ Institute of Computing Technology, Chinese Academy of Sciences, Beijing, China

² School of Biomedical Engineering, Suzhou Institute for Advanced Research,
University of Science and Technology of China, Suzhou, China

³ University of Chinese Academy of Sciences

⁴ Division of Life Sciences and Medicine, University of Science and Technology of
China, Hefei, Anhui, China

⁵ Department of Neurology, Institute on Aging and Brain Disorders, The First
Affiliated Hospital of USTC

Abstract. Clinical decision making requires counterfactual reasoning based on a factual medical image and thus necessitates causal image synthesis. To this end, we present a novel method for modeling the causality between demographic variables, clinical indices and brain MR images for Alzheimer’s Diseases. Specifically, we leverage a structural causal model to depict the causality and a styled generator to synthesize the image. Furthermore, as a crucial step to reduce modeling complexity and make learning tractable, we propose the use of low-dimensional latent feature representation of a high-dimensional 3D image, together with exogenous noise, to build causal relationship between the image and non-image variables. We experiment the proposed method based on 1586 subjects and 3683 3D images and synthesize counterfactual brain MR images intervened on certain attributes, such as age, brain volume and cognitive test score. Quantitative metrics and qualitative evaluation of counterfactual images demonstrates the superiority of our generated images.

Keywords: Image synthesis · Causal modeling · Brain MR.

1 Introduction

Clinical decision making heavily relies on pattern contrasting and longitudinal comparison of medical images. Despite countless medical images are taken everyday, these factual images fail to answer the following questions, say in brain MR imaging: *What would the brain image look like if the subject did not have Alzheimer’s Disease? What would be the changes of lateral ventricle in MR images if taken aspirin a month ago?* This kind of inquiry involves images in situations contradicting with the fact, *i.e.*, **counterfactual** [1], and necessitates **causal image synthesis** (CIS).

Although image synthesis has been explored extensively, existing image synthesis methods are correlation-based; yet the questions related to counterfactual images need to be answered with causality model to describe how demographic variables, disease variables and medical images interact with each other. Pearl

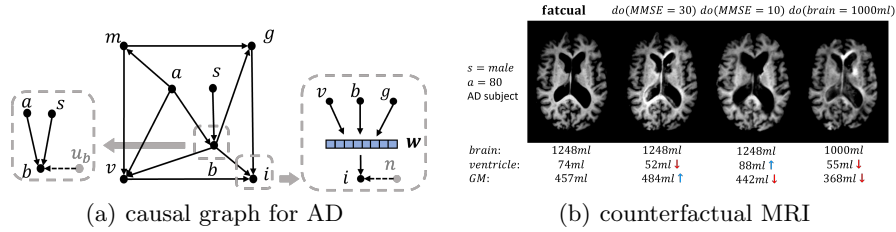


Fig. 1. (a) The causal graph for MRI for AD. Variables are image (i), age (a), sex (s), Mini Mental Sate Examination(MMSE) score (m) and brain (b), ventricle (v), grey matter (g) volumes. (b) The counterfactual MRI results, set score and brain volume.

proposes a structural causal model (SCM) [1] which utilises a directed acyclic graph (DAG) whose nodes represent the variables and edges point from causes to effect. Take Figure 1(a) as an example, node a (age) is a causal parent of node v (ventricle volume), which indicates the causal effect of age on brain ventricle (increasing age causes enlarged brain ventricle). SCM has been successful in epidemiology, econometrics and medicine [2,3,4] where the variables are in low-dimension in most cases.

However, causal image synthesis requires handling high-dimensional image data. Furthermore, 3D medical images, *e.g.*, CT, MRI, are even more challenging because of the computational demand, which leads to far less research, not to mention incorporating causality. Despite computational intractability, 3D images can provide much more information for clinical analysis. In addition, many attributes, *e.g.*, volume, topological connectivity, can only be calculated in 3D. Thus, constructing a causal medical image synthesis model in 3D is of great importance yet challenging. In this work, we attempt to bridge such a gap.

We choose Alzheimer’s Disease (AD) as the scenario. AD is the most common type of dementia and involves the atrophy of brain, which can be reflected in MR images. Besides, the causality in AD is of plenty of research which can provide our model with prior knowledge. We manage to synthesize brain MRI in 3D while handling the causal relationships between demographic variables, clinical disease variables and MR images. This model makes it possible to (i) sample and generate controllable life-like 3D brain MR images and (ii) answer the aforementioned counterfactual questions based on existing images. Fig. 1(b) shows the synthesised counterfactual MRI in the situation of the subject without AD or with a smaller brain, which contradicts with the fact.

Our contributions are in two folds. First, we propose a novel CIS model to generate controllable and counterfactual 3D brain MR images which can be evaluated by several metrics to ensure the reliability. To the best of our knowledge, it marks the first CIS attempt in 3D. Second, we shed light on the relationships between demographic, disease variables and MR images for AD patients.

2 Related Work

Our work is mostly related to medical image synthesis for disease modeling and other downstream tasks. A few works utilised causality for deep generative model to synthesize medical images for disease modeling [8], classification [9], segmentation [10], but they concentrate on 2D images and lack effective metrics to evaluate the quality of synthesised images. As for 3D images synthesis, there have been works for unpaired domain translation [11], low-dose CT denoising [12], super-resolution [13], brain tumor segmentation [14] and memory-efficient GAN-based model [15]. However, these 3D image generative models are designed for special tasks and lacks assumptions about causal structures thus are fundamentally limited for unable to generate causal images.

Causality in medical image analysis is also related to our work. There has been works [6,7] to emphasize the importance of causality for data scarcity and mismatch, fairness, domain generalization. Very limited works analyse the causality between geographical or disease variables and medical images mainly because the lack of meta-data and the insufficiency of data images themselves contain. Jiao *et al.* [16] discuss the causality between genetic data and Alzheimer’s Disease MRI data. Reinhold *et al.* [8] discuss the causal relationships in Multiple Sclerosis (MS) to make counterfactual predictions. However, the focus of our work is to generate causally controlled images instead of causality discovery, which allows us to apply prior medical and causality knowledge.

3 Methods

In this section, we first introduce SCM briefly and then the 3D StyleGAN model we use to generate MR images. Next, we explain how to combine the two to model the causality in AD and generate counterfactual MR images.

3.1 Structural causal model

A structural causal model (SCM) [1] specifies a set of observed variables \mathbf{V} , corresponding unobserved exogenous noise \mathbf{U} distributed according to $P(\mathbf{U})$ and a set of functions \mathbf{F} , in which f_i is the causal mechanism that generates v_i by $v_i = f_i(pa_i, u_i)$ with the causal parent of v_i as pa_i and u_i the unobserved noise. A directed acyclic graph (DAG) can represent an SCM by representing variables as nodes and causal effect as edges, as illustrated in Fig. 1(a).

For a given SCM, $\mathbf{M} = \langle \mathbf{U}, \mathbf{V}, \mathbf{F}, P(\mathbf{U}) \rangle$, under several assumptions [1], Pearl further provides the general solution for counterfactual inference. There are three steps: 1) *Abduction*: infer the unobserved noise \mathbf{U} with observed data \mathbf{V} and known functions \mathbf{F} ; 2) *Action*: Modify the graph \mathbf{M} according to desired intervention; and 3) *Prediction*: Compute counterfactuals $\tilde{\mathbf{V}}$ in the new graph.

Take the brain volume in Fig. 1(a) as an example. The observed variable brain volume (b) has two causal parents: age (a) and sex (s), which along with the unobserved noise u_b , decide the brain volume by $v_b = f_b(pa_b, u_b), pa_b =$

$\{v_a, v_s\}$. With causal mechanism f_b derived and $v_b = 1000 \text{ ml}$, $v_a = 50 \text{ years}$, $v_s = 0$ (*Female*) observed, to compute the counterfactual v'_b with age set to 40: 1) infer unobserved noise $p(u_b|e)$ with evidence $e = \{v_b = 1000, v_a = 50, v_s = 0\}$; 2) set $v'_a = 40$ and compute $p(v'_b) = \int p(v'_b|u_b, v_s, v'_a)p(u_b|e)du$.

3.2 Causality in AD

In order to generate causal MR images, firstly we need to model the causality in AD, *i.e.*, to derive the causal mechanism function $f_i \in \mathbf{F}$. As shown in Fig. 1(a), we constructed the causal graph in AD, referring to medical research about the causality effect of age or AD on brain, ventricle and grey matter(GM) volumes [30,31]. Atrophy of brain and enlarged ventricle are observed for increasing age, however, the process is accelerated radically for patients with AD, especially for the areas responsible for memory and language, mostly grey matter. We also conduct simple experiments on dataset to verify the causality, see Fig. 3(a) for an example.

In Fig. 1(a), the geographical variables sex and age have no causal parents therefore only need to be sampled from a prior distribution. Mini Mental Sate Examination(MMSE), which is denoted by node m in the graph, is a cognitive test widely used in clinical for AD. The score $m \in [0, 30]$ and a lower score indicates more cognitive impairment while health group usually score above 28.

The f_i for image i is modeled by the 3D styled generator, for the f_i except image, we assume that

$$v_i = \text{CondAffine}_\theta(u_i), u_i \sim \mathcal{N}(0, 1) \quad (1)$$

$\text{CondAffine}_\theta(\cdot)$ is an affine transform, whose parameters $\theta = \mathbf{g}_i(pa_i)$ is a learnable, fully-connected network (FCN). Reinhold *et al.* [8] use normalizing flows (NFs) to represent f_i which is more flexible but likely to overfit.

Our assumption can be expressed in another way:

$$v_i \sim \mathcal{N}(h_1(pa_i), h_2(pa_i)), h_1(\cdot) \text{ and } h_2(\cdot) \text{ are FCNs.} \quad (2)$$

Take v_b in Fig. 1(a) as an example. For the population of female at age 60, their brain volumes satisfy a Normal distribution, whose mean and variance are determined by sex and age. For each individual, u_b (noise for v_b) can be viewed as the individual character and further decides the precise value of v_b .

Assume there are k observed variables except image in the causal graph and we have observed N samples, *i.e.*, N sets of $\{v_i\}$, $i = 1, \dots, k$. f_i are trained to maximize the probability for all variables and all samples.

$$\{f_1, f_2, \dots, f_k\} = \underset{f_i}{\text{argmax}} \sum_{i=1}^k \sum_N P(v_i|pa_i). \quad (3)$$

With f_i trained, counterfactual variables (except images) can be calculated as described in **3.1**. We put the formulas of the detailed abduction, action, and prediction for f_i in supplementary material.

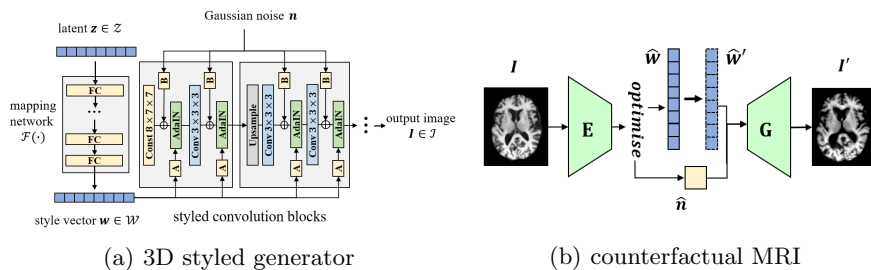


Fig. 2. (a) The structure of our 3D styled generator. (b) Counterfactual MRI synthesis. Notice that w changes but the unobserved exogenous noise n remains unchanged.

3.3 3D StyleGAN for MR image synthesis

StyleGAN [17] is a style-based generative adversarial network that has been proved successful for its astonishing quality of generated images. StyleGAN2 [23] achieves better performance for natural images, but previous works [21] indicate that StyleGAN is more suitable for 3D images because of the (De)Mod operators so our 3D styled generator is on the basis of StyleGAN [17].

A styled generator model, as in Fig. 2(a), consists of a mapping network \mathbf{F} and a series of styled convolution blocks. The mapping network \mathbf{F} maps latent $z \sim \mathcal{N}(\mathbf{0}, \mathbf{I}_n)$ to w . The styled convolution blocks \mathbf{G} then map w to image \mathbf{I} with Gaussian noise n added, *i.e.*,

$$\mathbf{I} = \mathbf{G}(w, n), \text{ where } w = \mathbf{F}(z). \quad (4)$$

To modify StyleGAN for 3D image, we use 3D convolutions and change the feature map depths due to computation consideration. Like StyleGAN[17], we apply a progressive training method: train for low resolution images firstly then increase for each phase. From the beginning at $8 \times 7 \times 7$, we finally generate images of $256 \times 224 \times 224$ at a 0.8mm isotropic resolution. By contrast, S. Hong *et al.*[21] also design a 3D StyleGAN but synthesize acceptable images of $80 \times 96 \times 112$ at a 2mm resolution finally. The details of model and training can be found in the open source code ⁶.

3.4 Counterfactual image generating using styleGAN

The causality between variables except image has been introduced in Section 3.2. As shown in Fig. 1(a), brain (b), ventricle (v), grey matter (g) volumes are the causal parents of image (i). However, directly using the high-dimensional 3D image in SCM adds modeling complexity and makes the modeling intractable.

As introduced in Section 3.3, a styled generator first maps a simple Gaussian distribution space \mathcal{Z} to \mathcal{W} by $\mathbf{F}(\cdot)$ and then from \mathcal{W} to image space \mathcal{I} by $\mathbf{G}(\cdot)$. Although the training is unsupervised, many previous works have demonstrated

⁶ <https://anonymous.4open.science/r/CausalMRI-488C/>

the intriguing disentangled and semantic properties of \mathcal{W} space both in natural image [18,19] and medical image domain [20,29]. The disentanglement and relatively low dimension of \mathcal{W} space provide advantages for performing image manipulation.

Inspired by the discussion in [17], we assume that \mathbf{w} control the basic continuous feature such as volumes in image \mathbf{i} while noise \mathbf{n} contributes to the sophisticated details, such as superficial sulcus and gyrus, as in Fig. 1(a). We verify the assumption by experiments in Section 4.3. Thus, we can preserve the character of a brain by \mathbf{n} and bridge causality between volumes and \mathbf{w} .

To generate counterfactual MR images, as illustrated in Fig. 2(b), we need to map images \mathbf{I} reverse to $\hat{\mathbf{w}}$ and $\hat{\mathbf{n}}$ with a fixed well-trained styled generator \mathbf{G} . We sample in the latent \mathcal{Z} space and obtain a set of \mathbf{w} and corresponding images \mathbf{I} . Then we train an encoder based on a pre-trained 3D ResNet50 [28] on the synthesized dataset by supervision in \mathcal{W} space. Further optimisation is conducted for $\hat{\mathbf{w}}$ and $\hat{\mathbf{n}}$ by supervision in \mathcal{I} space with an L_1 loss $|\mathbf{I} - \mathbf{G}(\hat{\mathbf{w}}, \hat{\mathbf{n}})|$. Then inspired by [29] that utilizes a Sigmoid function for classification, we train a linear regression $y = \boldsymbol{\alpha}^T \hat{\mathbf{w}} + \beta$ for the volume y and the encoded style vector $\hat{\mathbf{w}}$ to model the causality between volumes and \mathbf{w} .

Now we are ready to generate counterfactual image \mathbf{I}' (*set volume = y'*) from a factual image \mathbf{I} (*volume = y*) by following three steps: 1) map \mathbf{I} reverse to $\hat{\mathbf{w}}$ and $\hat{\mathbf{n}}$; 2) move $\hat{\mathbf{w}}$ along the direction of $\boldsymbol{\alpha}$ as volume changes; and 3) put $\hat{\mathbf{w}}'$ and $\hat{\mathbf{n}}$ into the fixed styled generator to generate the counterfactual image \mathbf{I}' .

$$\hat{\mathbf{w}}' = \hat{\mathbf{w}} + \frac{(y' - y)}{\|\boldsymbol{\alpha}\|} \boldsymbol{\alpha}, \quad \mathbf{I}' = \mathbf{G}(\hat{\mathbf{w}}', \hat{\mathbf{n}}). \quad (5)$$

Formulas for changing multiple volumes simultaneously are in the supplement. Intervention of other variables will affect the three volumes first and then image as they are causal parents.

4 Experiments

4.1 Dataset

We used brain MR T1 images from two publicly available datasets: ADNI [34] and OASIS [32,33]. All images are skull-stripped by FSL [26], registered to MNI152 space and resampled to a 0.8mm isotropic resolution by ANTs [25], and trimmed to $256 \times 224 \times 224$. We then segment the processed MR images and obtain grey matter volume by ANTs and ventricle volume by a trained CNN model [27]. Meta-data of sex, age, and MMSE score (introduced in section 3.2) are provided by the dataset. Both healthy individuals (Health Control, HC) and cognitive impaired individuals (cognitive Impaired, CI) are included and there are multiple MR scans for every subject for at least a 6-month interval. Totally there are 1586 subjects (440 CI) and 3683 images (834 CI).

Table 1. $\log(p(v_i|pa_i))$ on average. Test on OASIS2

	Brain volume	Ventricle volume	GM volume	Score
Normalising Flow	-1.42	-1.50	-1.21	-0.98
Conditional Affine (ours)	-1.41	-1.32	-1.10	-2.38

4.2 Causality in AD

As discussed in Section 3.2, we use $CondAffine_{\theta}(\cdot)$, $\theta = \mathbf{g}_i(pa_i)$, a learnable FCN to model the causality between variables except image. We train on OASIS3 (2275 images), validate on OASIS2 (373 images), and test on ADNI1 (1035 images). Compared with Normalising Flow used by [5,8], our method can avoid overfitting and better generalise as Table 1 shows. Results on training and validation datasets are in the supplementary materials. For MMSE score, we believe that only age and sex are insufficient to generate the distribution, more such as genetic data is needed. Fig. 3(a) shows the true and predicted distribution of MMSE score and ventricle volume on test dataset.

4.3 Synthesized 3D MRI quality

General synthesized image evaluation We evaluate the synthesised images by Fréchet Inception Distance (FID) and Maximum Mean Discrepancy (MMD). Lower values of FID/MMD indicate that the distributions of synthesised images are closer to real ones. As shown in Table 2, our model is compared with the state-of-the-art 3D image generator HA-GAN [15] and a styleGAN model by Hong et al. [21]. Since they use different metrics, we take the numbers they report and compare our model with them, respectively. Figure 3(b) shows a sample and more are presented in the supplementary material. The results prove our model can generate realistic images comparable with the-state-of-art model. We also request a clinician with over 30 years of brain image reading experience to recognize if an image is real or synthesized for 50 randomly selected images. His recognition accuracy is 50%, exactly like flipping a fair coin.

Table 2. Image quality evaluation. HA-GAN uses a pretrained 3D ResNet [28] to extract features and compute FID and MMD, while Hong et al.[21] compute MMD in images in miniBatch and FID of the middle slice of images (S: Sagittal, A: Axial, and C: Coronal).

	FID	MMD		bMMD ²	FID-S	FID-A	FID-C
HA-GAN [15]	.004(.001)	.086(.029)	Hong et al. [21]	4497(898)	106.9	71.3	90.2
ours	.010(.001)	.024(.001)	ours	1109(37)	57.5	46.9	67.1

Counterfactual image synthesis. The counterfactual images are evaluated for (1) whether they change according to the set volume, and (2) whether they

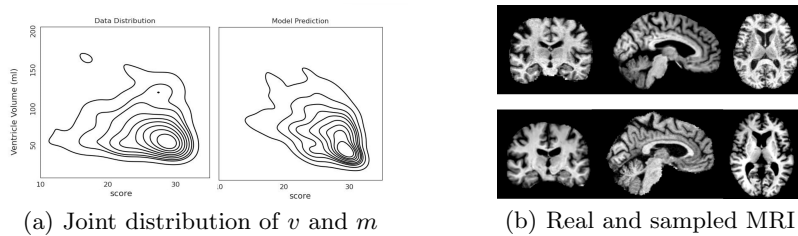


Fig. 3. (a) The joint distribution of score and ventricle volume. Negative correlation can be observed. (b) Real MRI (the first row) and synthesized MRI (the second row) sampled from our generator.

preserve the characteristic structure of brain. We adjust the volumes by $\pm 15\%$, generate counterfactual image, calculate the volumes, and measure the SSIM between \mathbf{I}' and \mathbf{I} .

Table 3. Metrics for counterfactual MRI. Randomly choose 500 MRI each test, generate counterfactual MRI and compute the mean and std of the changes of volumes.

Setting	-15%	-10%	-5%	+5%	+10%	+15%
Actual Change						
Brain volume	-0.13(.02)	-0.11(.01)	-0.06(.01)	0.06(.01)	0.12(.01)	0.17(.02)
GM volume	-0.13(.03)	-0.09(.01)	-0.04(.01)	0.03(.01)	0.08(.03)	0.12(.04)
Ventricle volume	-0.20(.08)	-0.13(.05)	-0.07(.01)	0.05(.01)	0.10(.03)	0.15(.07)
SSIM						
Brain volume	0.78(.05)	0.85(.04)	0.92(.02)	0.93(.02)	0.87(.03)	0.81(.04)
GM volume	0.84(.04)	0.89(.03)	0.94(.02)	0.93(.02)	0.86(.04)	0.78(.05)
Ventricle volume	0.94(.03)	0.95(.02)	0.96(.01)	0.96(.01)	0.96(.02)	0.95(.03)

As Table 3 shows, the brain volume changes most accurately possibly because brain is the largest (average $1354ml$) compared with grey matter ($527ml$) and ventricle ($41ml$). SSIM between 2 random real images is $0.71(.001)$ and the SSIM between 2 images of the same individual (interval > 1 year) is $0.85(.05)$, which proves that counterfactual MRI preserves the characteristic structure. Figure 1(b) visualizes counterfactual MR images. We set $MMSE = 30$ for an AD patient to answer the question *What would the brain image look like if the subject did not have Alzheimer’s Disease?* Results show a smaller ventricle and a larger grey matter volume, in accordance with the medical research on AD [30,31]. We also show how the image would look like if the illness is more severe ($MMSE = 10$) or if the subject has a smaller brain (brain volume = $1000ml$). See more results in supplementary material.

5 Conclusion

This work presents a novel method for causal image synthesis in 3D. We combine structural causal model and 3D StyleGAN to depict the causality in AD and evaluate the reliability of the counterfactual images. Our work still have some limitations. The \mathcal{W} space is incapable to encode small areas such as hippocampus. This may be improved by adding supervision when training the styled generator to help \mathcal{W} space learn more information. A better image generator, *e.g.*, diffusion model may also address this problem.

In spite of the limitations, we believe this work has shed light on a new area: causal image synthesis. Apart from contributions to clinical analysis, a causal image synthesis model can also help to understand the relationships between images and clinical indicators. Besides, this model can augment dataset for other downstream tasks by providing controlled data as supplement, so as to benefit other image analysis model or address data bias problem.

References

1. Pearl, J.: Causality. 2nd edn. Cambridge University Press (2009)
2. Parascandola, M., Douglas L.: Causation in epidemiology. *Journal of Epidemiology & Community Health* **55**(12), 905–912 (2001)
3. Herman O. A. Wold.: Causality and econometrics. *Econometrica* **22**(2), 162–177 (1954)
4. Kuipers, B., Kassirer, J. P.: Causal reasoning in medicine: analysis of a protocol. *Cognitive Science* **8**(4), 363–385 (1984)
5. Pawlowski, N., Coelho de Castro, D., Glocker, B.: Deep structural causal models for tractable counterfactual inference. In: *Advances in Neural Information Processing Systems*. pp. 857–869 (2020)
6. Castro, D.C., Walker, I., Glocker, B.: Causality matters in medical imaging. *Nature Communications* **11**(1), 1–10 (2020)
7. Vlontzos, A., Rueckert, D., Kainz, B.: A review of causality for learning algorithms in medical image analysis. *arXiv preprint arXiv:2206.05498* (2022)
8. Reinhold, J. C., Carass, A., Prince, J. L.: A structural causal model for MR images of multiple sclerosis. In: *International Conference on Medical Image Computing and Computer-Assisted Intervention*. pp. 782–792. Springer (2020)
9. Kumar, A., Hu, A., Nichyporuk, B., Falet, J. P. R., Arnold, D. L., Tsaftaris, S., Arbel, T.: Counterfactual image synthesis for discovery of personalized predictive image markers. In: *Artificial Intelligence over Infrared Images for Medical Applications and Medical Image Assisted Biomarker Discovery: MICCAI Workshop*. pp. 113–124. Springer (2022)
10. Sanchez, P., Kascenas, A., Liu, X., O’Neil, A. Q., Tsaftaris, S. A.: What is healthy? generative counterfactual diffusion for lesion localization. In *Deep Generative Models: Second MICCAI Workshop DGM4MICCAI*. pp. 34–44. Springer (2022)
11. Uzunova, H., Ehrhardt, J., Handels, H.: Memory-efficient GAN-based domain translation of high resolution 3D medical images. *Computerized Medical Imaging and Graphics* **86**, 101801

12. Shan, H., Zhang, Y., Yang, Q., Kruger, U., Kalra, M.K., Sun, L., Cong, W., Wang, G.: 3-D convolutional encoder-decoder network for low-dose CT via transfer learning from a 2-D trained network. *IEEE Transactions on Medical Imaging*, **37**(6), pp. 1522–1534 (2018)
13. Kudo, A., Kitamura, Y., Li, Y., Iizuka, S., Simo-Serra, E.: Virtual thin slice: 3D conditional GAN-based super-resolution for CT slice interval. In: *MICCAI Machine Learning for Medical Image Reconstruction: Second International Workshop*. pp. 91–100. Springer (2019)
14. Cirillo, M. D., Abramian, D., Eklund, A.: Vox2Vox: 3D-GAN for brain tumour segmentation. In: *MICCAI Brainlesion Workshop*. pp. 274–284. Springer (2020)
15. L. Sun, J. Chen, Y. Xu, M. Gong, K. Yu, K. Batmanghelich.: Hierarchical Amortized GAN for 3D High Resolution Medical Image Synthesis. *IEEE Journal of Biomedical and Health Informatics* **26**(8), 3966–3975 (2022)
16. Jiao, R., Lin, N., Hu, Z., Bennett, D. A., Jin, L., Xiong, M.: Bivariate causal discovery and its applications to gene expression and imaging data analysis. *Frontiers in genetics* **9**, 347 (2018)
17. Karras, T., Laine, S., Aila, T.: A style-based generator architecture for generative adversarial networks. In: *Proceedings of the IEEE Conference on Computer Vision and Pattern Recognition*. pp. 4401–4410 (2019)
18. Shen, Y., Gu, J., Tang, X., Zhou, B.: Interpreting the latent space of gans for semantic face editing. In *Proceedings of the IEEE conference on Computer Vision and Pattern Recognition*. pp. 9243–9252 (2020)
19. Shukor, M., Yao, X., Damodaran, B. B., Hellier, P.: Semantic Unfolding of Stylegan Latent Space. In: *IEEE International Conference on Image Processing (ICIP)*. pp. 221–225 (2022)
20. Daroach, G. B., Duenweg, S. R., Brehler, M., Lowman, A. K., Iczkowski, K. A., Jacobsohn, K. M., Yoder, J. A., LaViolette, P. S.: Prostate Cancer Histology Synthesis Using StyleGAN Latent Space Annotation. In: *Medical Image Computing and Computer Assisted Intervention*. pp. 398–408. Springer (2022)
21. Hong, S., Marinescu, R., Dalca, A. V., Bonkhoff, A. K., Bretzner, M., Rost, N. S., Golland, P.: 3d-stylegan: A style-based generative adversarial network for generative modeling of three-dimensional medical images. In *Deep Generative Models, and Data Augmentation, Labelling, and Imperfections: DGM4MICCAI Workshop*. pp. 24–34. Springer (2021)
22. Hara, K., Kataoka, H., Satoh, Y.: Can spatiotemporal 3d cnns retrace the history of 2d cnns and imagenet? In: *Proceedings of the IEEE Conference on Computer Vision and Pattern Recognition*. pp. 6546–6555 (2018)
23. Karras, T., Laine, S., Aittala, M., Hellsten, J., Lehtinen, J., Aila, T.: Analyzing and improving the image quality of stylegan. In: *Proceedings of the IEEE Conference on Computer Vision and Pattern Recognition*. pp. 8110–8119 (2020)
24. Schutte, K., Moindrot, O., Hérent, P., Schiratti, J. B., Jégou, S.: Using stylegan for visual interpretability of deep learning models on medical images. *arXiv preprint arXiv:2101.07563* (2021)
25. Avants, B.B., Tustison, N., Song, G.: Advanced normalization tools (ANTS). *Insight J* **2**(365), 1–35 (2009)
26. Smith, S. M., Jenkinson, M., Woolrich, M. W., Beckmann, C. F., Behrens, T. E., Johansen-Berg, H., Bannister, P. R., Luca, M. D., Drobnjak I., Flitney, D. E., Niazy, R. K., Saunders, J., Vickers, J., Zhang, Y., Stefano N. D., Brady, J. M., Paul, Matthews, P. M.: Advances in functional and structural MR image analysis and implementation as FSL. *Neuroimage* **23**, S208–S219 (2004)

27. Shao, M., Han, S., Carass, A., Li, X., Blitz, A. M., Shin, J., Prince, J., L., Ellingsen, L. M.: Brain ventricle parcellation using a deep neural network: Application to patients with ventriculomegaly. *NeuroImage: Clinical* **23**, 101871 (2020)
28. Chen, S., Ma, K., Zheng, Y.: Med3d: Transfer learning for 3d medical image analysis. arXiv preprint arXiv:1904.00625 (2019)
29. Schutte, K., Moindrot, O., Hérent, P., Schiratti, J. B., Jégou, S.: Using stylegan for visual interpretability of deep learning models on medical images. arXiv preprint arXiv:2101.07563 (2021)
30. Yi, H. A., Möller, C., Dieleman, N., Bouwman, F. H., Barkhof, F., Scheltens, P., Flier, W. M., Vrenken, H.: Relation between subcortical grey matter atrophy and conversion from mild cognitive impairment to Alzheimer’s disease. *Journal of Neurology, Neurosurgery & Psychiatry*, **87**(4), 425–432 (2016)
31. Nestor, S. M., Rupsingh, R., Borrie, M., Smith, M., Accomazzi, V., Wells, J. L., Fogarty, J., Bartha, R., Alzheimer’s Disease Neuroimaging Initiative.: Ventricular enlargement as a possible measure of Alzheimer’s disease progression validated using the Alzheimer’s disease neuroimaging initiative database. *Brain*, **131**(9), 2443–2454 (2008)
32. OASIS-2: Longitudinal: <https://doi.org/10.1162/jocn.2009.21407>
33. OASIS-3: Longitudinal Multimodal: <https://doi.org/10.1162/jocn.2009.21407>
34. ADNI1: <https://adni.loni.usc.edu/>